Comparison of Two-Equation Model and Reynolds Stress Models with Experimental Data for the Three-Dimensional Turbulent Boundary Layer in a 30 Degree Bend

Insub Lee and Hong Sun Ryou*
(Chung-Ang University)
Seong Hyuk Lee
(Research Institute of Production Engineering, Chung-Ang University)
Soo Chae
(Kun-Jang College)

The objective of the present study is to investigate the pressure-strain correlation terms of the Reynolds stress models for the three dimensional turbulent boundary layer in a 30° bend tunnel. The numerical results obtained by models of Launder, Reece and Rodi (LRR), Fu and Speziale, Sarkar and Gatski (SSG) for the pressure-strain correlation terms are compared against experimental data and the calculated results from the standard k-ε model. The governing equations are discretized by the finite volume method and SIMPLE algorithm is used to calculate the pressure field. The results show that the models of LRR and SSG predict the anisotropy of turbulent structure better than the standard k-ε model. Also, the results obtained from the LRR and SSG models are in better agreement with the experimental data than those of the Fu and standard k-ε models with regard to turbulent normal stresses. Nevertheless, LRR and SSG models do not effectively predict pressure-strain redistribution terms in the inner layer because the pressure-strain terms are based on the locally homogeneous approximation. Therefore, to give better predictions of the pressure-strain terms, non-local effects should be considered.

Key Words : Pressure-Strain Correlation Terms, Reynolds Stress Model (RSM), Three Dimensional Turbulent Boundary Layer (3DTBL), Anisotropy, Turbulent Normal Stress.

1. Introduction

The 3DTBL can be observed in most engineering flows such as those over swept wings of aircraft, and those inside turbomachines. Particularly, when the spanwise pressure gradient exists, a skewing effect of flow resulting from this pressure gradient generates an additional mean velocity gradient $\partial W/\partial y$. This additional mean velocity gradient contributes to increase of production of turbulent kinetic energy, indicating that turbulent mixing is very high as the cross flow develops.

The previous experiments on the 3DTBL have been conducted by Bradshaw and Terrell (1969), Johnston (1970), Schwarz and Bradshaw (1992) and Flack and Johnston (1993). Previous numerical studies were done by Spalart (1988) and Durbin (1993).

To effectively predict velocity field and turbulence structure of this flow, it is important to use a turbulence model which is capable of accurately

* Corresponding Author, **E-mail** : cfdmec@cau.ac.kr
TEL : +82-2-813-3669 ; **FAX** : +82-2-814-9476
Department of Mechanical Engineering, Chung-Ang University, 221, Heuksuk-dong, Dongjak-ku, Seoul 156-756, Korea. (Manuscript Received May 28, 1999 ; Revised September 11, 1999)

predicting the turbulent structure.

Two-equation turbulence models, such as the standard k-ε model, may not be appropriate for prediction of features of 3DTBL because the models are based on the isotropic assumption i. e. the shear stress vector is aligned with the velocity gradient vector and the normal stresses are roughly equal (Wilcox, 1993). However, according to Hogg and Leschziner (1989), Lin (1990) and Johnston (1994), the RSM predicts the anisotropy of turbulent intensities, the curvature effect and the secondary motion better than the isotropic eddy viscosity model. The RSM is suitable for describing the anisotropy of turbulent intensities since it directly calculates Reynolds stress transport equations and intrinsically is not based on the isotropic concept.

Although the RSM is suitable for prediction of 3DTBL, a number of researchers have pointed out some weaknesses of the RSM. Particularly, Fu (1988) argued that the improved modeling of pressure-strain redistribution terms is required to overcome the problems of quasi-isotropic assumption. Also, Schwarz and Bradshaw (1992) have pointed out that the non-local effect should be considered to predict redistributing effect of pressure-strain.

To develop a new model which effectively predicts turbulent structure, it is necessary to examine the characteristics of the models for the pressure-strain redistribution terms. Therefore, the main objectives of the present paper are to investigate the pressure-strain correlation terms and to give better understanding of the 3DTBL in a 30° bend. The models of Launder, Reece and Rodi (LRR) (1975), Fu (1988), Speziale, Sarkar and Gatski (SSG) (1991) are adopted in this paper to investigate the characteristics of pressure-strain redistribution terms. The calculated results from these models are compared with the experimental data obtained by Schwarz and Bradshaw (1992) and the calculated results from the standard k-ε model (Jones and Launder, 1972).

2. Turbulence Models

2.1 Reynolds-stress models

The Reynolds-stress transport equations for steady, incompressible flows are written as follows.

$$U_k\frac{\partial}{\partial x_k}(\overline{u_iu_j}) = P_{ij}+d_{ij}+\phi_{ij}-\varepsilon_{ij} + \frac{\partial}{\partial x_k}\left(\nu\frac{\partial \overline{u_iu_j}}{\partial x_k}\right) \tag{1}$$

where P_{ij} is the production term, d_{ij} is the turbulent diffusion term, ϕ_{ij} is the pressure-strain redistribution term, and ε_{ij} is the dissipation term.

$$P_{ij} = -\left[\overline{u_iu_k}\frac{\partial U_j}{\partial x_k}+\overline{u_ju_k}\frac{\partial U_i}{\partial x_k}\right] \tag{2}$$

$$d_{ij} = \frac{\partial}{\partial x_k}\left[\frac{c_\mu}{\sigma_k}\frac{k^2}{\varepsilon}\frac{\partial \overline{u_iu_j}}{\partial x_k}\right] \tag{3}$$

$$\varepsilon_{ij} = \frac{2}{3}\delta_{ij}\varepsilon \tag{4}$$

Turbulent energy dissipation equation is

Table 1 Models of pressure-stain terms (LRR, Fu and SSG models)

	$\phi_{ij,1}$	$\phi_{ij,2}$
LRR model	$-c_1\varepsilon b_{ij}$	$c_2[\overline{u_iu_l}\frac{\partial U_j}{\partial x_l}+\overline{u_ju_l}\frac{\partial U_i}{\partial x_l})-\frac{1}{3}\delta_{ij}\overline{u_lu_m}\frac{\partial U_l}{\partial x_m}]$
Fu Model	$-\tilde{c}_1\varepsilon[a_{ij}+c_1'(a_{ij}^2-\frac{1}{3}\delta_{ij}A_2)]-\varepsilon a_{ij}$	$-0.6(P_{ij}-\frac{1}{3}\delta_{ij}P_{kk})+0.3a_{ij}\varepsilon(\frac{P_{kk}}{\varepsilon})$ $-0.2(R_{im}P_{mj}+R_{mj}P_{im})-0.4kR_{li}R_{kj}S_{lk}$ $-r[A_2(P_{ij}-D_{ij})+3a_{li}a_{kj}(P_{lk}-D_{lk})]$
SSG model	$-(c_1\varepsilon+c_1^*P)b_{ij}+c_2\varepsilon(b_{ik}b_{kj}-\frac{1}{3}b_{mn}b_{mn}\delta_{ij})$	$(c_3-c_3^*\Pi^{0.5})kS_{ij}$ $-c_4k(b_{ik}S_{jk}+b_{jk}S_{ik}-\frac{2}{3}b_{mn}S_{mn}\delta_{ij})$ $-c_5k(b_{ik}W_{jk}+b_{jk}W_{ik})$

Table 2 Coefficients in the LRR model

C_1	C_2	C_{w1}	C_{w2}
1.8	0.6	0.5	0.3

Table 3 Coefficients in the SSG and Fu models

$\tilde{C}_1$	C_1'	C_1	C_1^*	C_2	C_3	C_3^*	C_4	C_5
$7.5A^{0.5}A_2$	0.6	3.8	1.8	4.2	0.8	1.3	1.25	0.4

Table 4 Coefficients in the standard k-ε model

$C_{\varepsilon 1}$	$C_{\varepsilon 2}$	σ_k	σ_ε
1.44	1.92	1.0	1.3

$$\rho U_j\frac{\partial \varepsilon}{\partial x_j}=C_{\varepsilon 1}\frac{\varepsilon}{k}\left(-\rho\overline{u_i'u_j'}\frac{\partial U_i}{\partial x_j}\right)-C_{\varepsilon 2}\frac{\rho\varepsilon^2}{k}+\frac{\partial}{\partial x_j}\left(\left(\mu+\frac{\mu_t}{\sigma_\varepsilon}\right)\frac{\partial \varepsilon}{\partial x_j}\right) \tag{5}$$

The LRR model which is listed in Table 1 combines the linear Rotta (1979) model for the slow part of the pressure strain term with a linear model for the rapid part. The experimental coefficients were given by Gibson and Launder (1978). Also, the equation for wall correction near the wall is written as follows.

$$\phi_{ij,w}=C_{w1}\frac{\varepsilon}{k}\left[\overline{u_k'u_m'}n_kn_m\delta_{ij}-\frac{3}{2}\overline{u_k'u_i'}n_kn_j-\frac{3}{2}\overline{u_k'u_j'}n_kn_i\right]f+C_{w2}\frac{\varepsilon}{k}\left[\phi_{km,2}n_kn_m\delta_{ij}-\frac{3}{2}\phi_{ik,2}n_kn_j-\frac{3}{2}\phi_{kj,2}n_kn_i\right]f \tag{6}$$

The coefficients used in the LRR model are summarized in Table 2.

The Fu (1988) model uses a quadratic model for the slow part of the pressure strain term and a cubic quasiisotropic model (CQIM) for the rapid part. The SSG model uses a quadratic model for the slow part of the pressure-strain term that has been calibrated against return-to-isotropy data. The model for the rapid part of the pressure-strain term is based on a dynamical systems analysis constrained by consistency with the rapid distortion theory and experiments on homogeneous shear flows. The equations for Fu and SSG models are represented in Table 1 and then coefficients are written in Table 3.

2.2 The standard k-ε model

The transport equations of turbulent kinetic energy and dissipation are as follows.

$$\rho U_l\frac{\partial k}{\partial x_l}=-\rho\overline{u_iu_j}\frac{\partial U_i}{\partial x_j}+\frac{\partial}{\partial x_l}\left(\left(\mu+\frac{\mu_t}{\sigma_k}\right)\frac{\partial k}{\partial x_l}\right)-\rho\varepsilon \tag{7}$$

$$\rho U_l\frac{\partial \varepsilon}{\partial x_l}=C_{\varepsilon 1}\frac{\varepsilon}{k}\left(-\rho\overline{u_i'u_j'}\frac{\partial U_i}{\partial x_j}\right)-C_{\varepsilon 2}\frac{\rho\varepsilon^2}{k}+\frac{\partial}{\partial x_l}\left(\left(\mu+\frac{\mu_t}{\sigma_\varepsilon}\right)\frac{\partial \varepsilon}{\partial x_l}\right) \tag{8}$$

where $C_{\varepsilon 1}$, $C_{\varepsilon 2}$, σ_k and σ_ε are constants used in the model. Their values represented in Table 4.

3. Numerical Approach and Boundary Conditions

The governing equations without boundary layer simplifications are solved by the finite volume method on a staggered grid system. Scalar quantities are stored at the center of the scalar control volume, and other quantities are stored at the cell faces. The SIMPLE algorithm is adopted in the present solution procedure to provide solution for the pressure field.

The inlet boundary conditions for mean velocity, normal stress, shear stress $-\rho\overline{u'v'}$, and dissipation are given from the experimental data (Schwarz and Bradshaw, 1992) and the other shear stresses $-\rho\overline{u'w'}$, $-\rho\overline{v'w'}$ are zero because initial flow is 2DTBL. In the outlet boundary conditions, the streamwise derivatives of the dependent variables are assumed to be negligible at exit. In the wall boundary conditions, a possible approach to resolve the region $y^+<50$ is to use a low-Reynolds-number model, but this approach is too costly. The alternative is to adopt the wall-function approach of Launder and Spalding (1974). In the present calculation, the wall functions are used to bridge the near wall region as follows.

$$\tau_w=\frac{\rho C_\mu^{1/4}k_p^{1/2}\varkappa U_p}{\ln(Ey_p^+)} \tag{9}$$

where y_p^+ is defined as

$$y_p^+=\frac{\rho C_\mu^{1/4}k_p^{1/2}y_p}{\mu} \tag{10}$$

The subscript p refers to the first nodal point

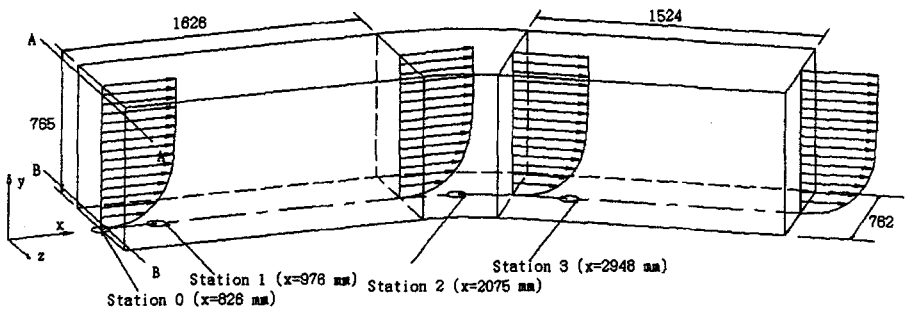

Fig. 1 Schematic diagram of computational domain

adjacent to the wall and χ is von Karman constant.

The steep gradients of both mean-flow and turbulence quantities also necessitate modification of the turbulent transport equations. The present approach is based on the two-layers methodology (Launder, 1986). Since the near-wall energy-dissipation rate is not determined from the related ε equation, ε at the near-wall node P is determined as

$$\varepsilon_P = C_\mu^{3/4} \frac{k_P^{3/2}}{\chi y_P} \tag{11}$$

4. Results and Discussions

In this paper, to investigate the pressure-strain correlation terms of the Reynolds stress models, numerical computations are carried out in 3DTBL in a bend. Figure 1 is the schematic diagram of the computational domain. The flow can be divided into three regions. First region (Station 0 and Station 1) is a 2DTBL without pressure gradient. Second region (Station 2) is bend region where 2DTBL is gradually changed to 3DTBL by the spanwise pressure gradient. Final region (Station 3) is recovery region where the additional mean-strain rate due to pressure gradient decays and the flow eventually reverts to a 2DTBL. To examine the prediction capability of different models for characteristics of 3DTBL, the analysis and comparison of computed results are carried out at Stations 1 and 2 along the centerline as shown in Fig. 1. The results from the RSM and the standard k-ε model are compared with the experimental data of Schwarz and Bradshaw (1992).

Table 5 Grid system for grid independence test

	Case 1	Case 2	Case 3	Case 4
X	35	35	35	35
Y	30	55	70	100
Z	21	21	21	21

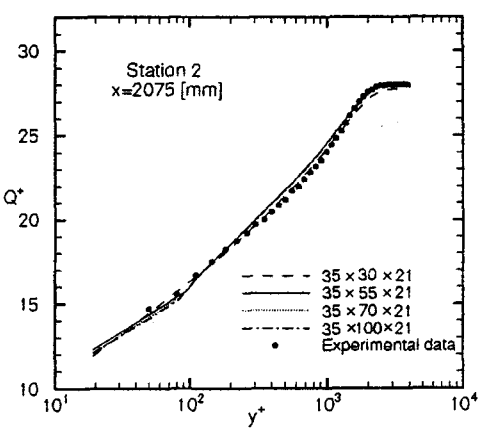

Fig. 2 Grid independence test (using LRR model)

Before the results of each model are compared, it is important to ascertain the grid convergence of the solution. Figure 2 shows the mean velocity obtained by using LRR model with the four different grid systems shown in Table 5. The grid number in z direction is consistently used to reduce the side wall effect as possible. As shown in Fig. 2, a $35 \times 21 \times 55$ (Case 2) grid system is adopted for all further numerical computations because Cases 3 & 4 do not yiell any improvement.

Figures 3(a) and (b) show streamlines obtained by using the LRR model in the free-stream region and the near wall region. Flow in near wall region is strongly deflected towards the

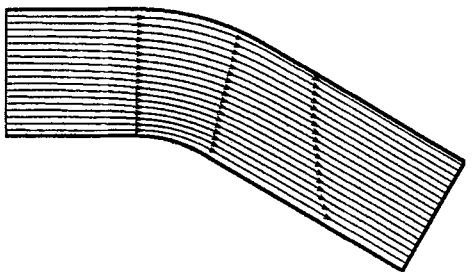

Fig. 3(a) Streamlines at free-stream region(A-A)

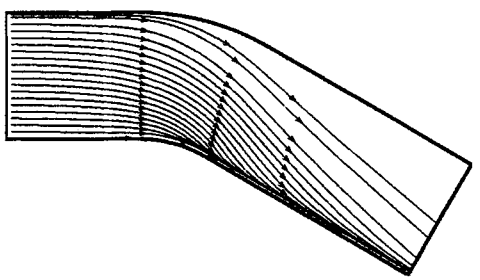

Fig. 3(b) Streamlines at near wall region(B-B)

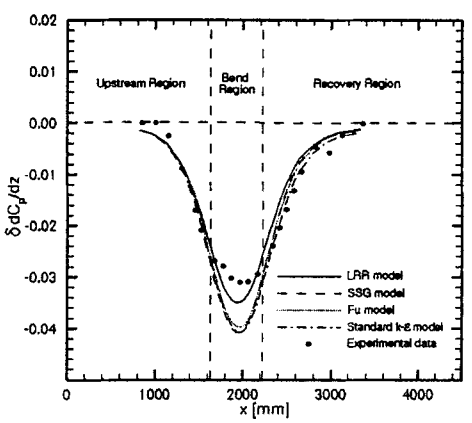

Fig. 4 Comparison of the spanwise pressure gradient

convex side wall of the bend by spanwise pressure gradient because the momentum in the near wall region is smaller than that in the free-stream region. In contrast, the calculated free-stream streamlines in Fig. 3(a) roughly follow the curvature of the bend.

Figure 4 compares the calculated non-dimensional spanwise pressure gradients along the centerline with the experimental data. The spanwise pressure gradient predicted by the LRR model is in good agreement with the experiment data. However, there is some disagreement

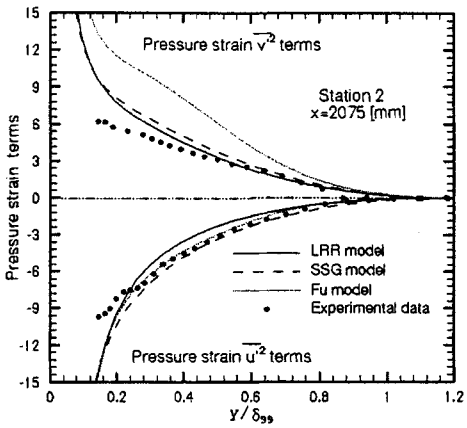

Fig. 5 Calculated results of pressure strain term

between the results of the SSG, Fu, and the standard k-ε model and experimental data.

Figure 5 shows the calculated results of pressure-strain redistribution terms in the $\overline{u'^2}$ stress transport equation and $\overline{v'^2}$ stress transport equation. The pressure-strain $\overline{u'^2}$ terms calculated by the LRR, SSG and Fu models agree closely with experimental data except near wall region. However, the pressure-strain $\overline{v'^2}$ terms calculated by the LRR and SSG models are slightly overpredicted, and those from the Fu model are considerably overpredicted. The sign of pressure-strain $\overline{u'^2}$ terms is in direct opposition to the generation term in the $\overline{u'^2}$ stress transport equation because the pressure work done by pressure-strain $\overline{u'^2}$ terms is given from deformation work done by production in the $\overline{u'^2}$ stress transport equation. Therefore, the pressure-strain $\overline{u'^2}$ term is negative for positive production in the $\overline{u'^2}$ stress transport equation. Also, the positive pressure-strain term of $\overline{v'^2}$ stress transport equation without production is generated by the negative pressure-strain $\overline{u'^2}$ term caused by redistribution effect of the pressure-strain term. The pressure-strain $\overline{v'^2}$ term of the Fu model is considerably overpredicted as shown in Fig. 5 because this model does not predict the redistribution term effectively. Also, this overprediction induces the overprediction of normal stress $\overline{v'^2}$ because the pressure-strain $\overline{v'^2}$ term contributes to the production of the $\overline{v'^2}$ stress transport equation. It can be seen in Fig. 5 that all of the models show good

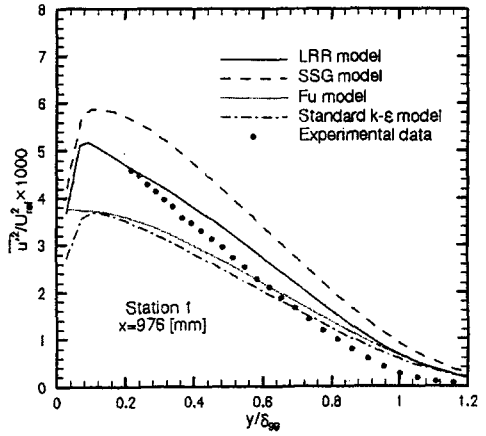

Fig. 6 Calculated results of normal stress $\overline{u'^2}$

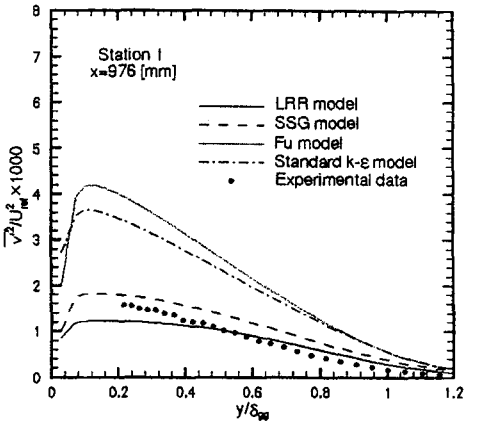

Fig. 7 Calculated results of normal stress $\overline{v'^2}$

prediction of pressure-strain redistribution terms in the outer layer, whereas they fail to predict pressure-strain redistribution terms in the inner layer. This failure may be due to the turbulent modeling for the pressure-strain term. In principle, the pressure-strain correlation is not a localized process, and involves contributions from every point in the flow. This would suggest that a two-point correlation is more appropriate. Nevertheless, most of models introduced earlier for pressure-strain correlation are based on the locally homogeneous approximation. Actually, Reynolds (1991) has developed models for the pressure-strain terms to incorporate global information of the turbulent flow into the pressure-strain term modeling by using the non-local concept. However, the adopted models in this paper are not capable of describing the non-local process existing in the inner layer since these models are intrinsically based on the local concept. To give better predictions of the pressure-strain term in the inner layer, a way to bring the non-local effect into the turbulence modeling for the pressure-strain term should be considered.

Figures 6 to 8 compare the distribution of turbulent normal stresses in the upstream region (Station 1). The normal stress $\overline{u'^2}$ of the LRR model is in better agreement with the experimental data than those of the SSG, Fu and standard k-ε models as noted in Fig. 6. The $\overline{v'^2}$ stress of the models of LRR and SSG closely agree with experimental data. In contrast, there are some

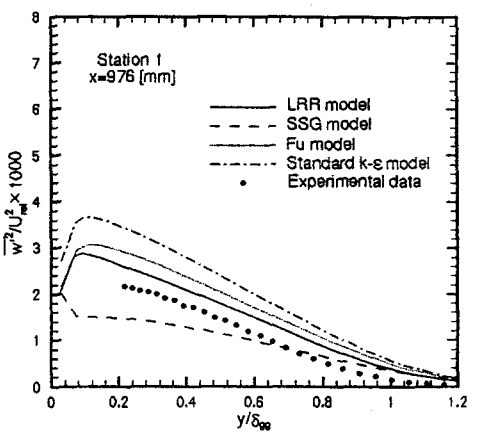

Fig. 8 Calculated results of normal stress $\overline{w'^2}$

discrepancies between the results of the Fu and standard k-ε models and the experimental data. According to Schwarz and Bradshaw (1992), the pressure-strain correlation terms predicted by several RSMs deviated from the experimental data, while the predicted turbulent diffusion terms were relatively closer to the experimental data. Therefore, as shown in Fig. 5, the $\overline{v'^2}$ stress overpredicted by the Fu model is due to the inaccurate prediction of the pressure-strain correlation. In particular, the standard k-ε model fails because this model is intrinsically based on the isotropic concept. It is seen from Fig. 8 that the LRR and SSG models perform better than the Fu and standard k-ε models in the prediction of the $\overline{w'^2}$ stress.

Figures 9 to 11 present the comparison of the

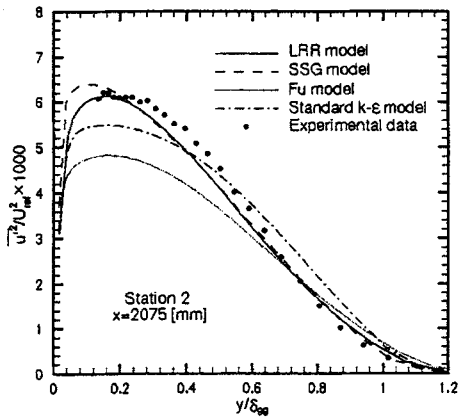

Fig. 9 Calculated results of normal stress $\overline{u'^2}$

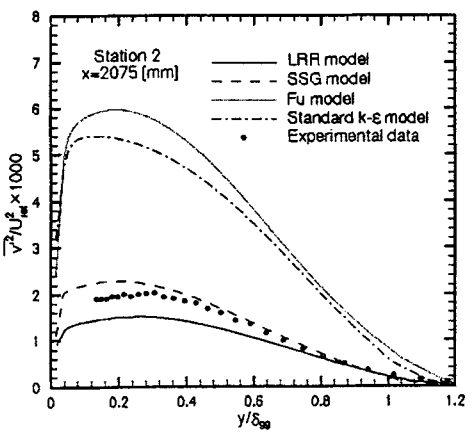

Fig. 10 Calculated results of normal stress $\overline{v'^2}$

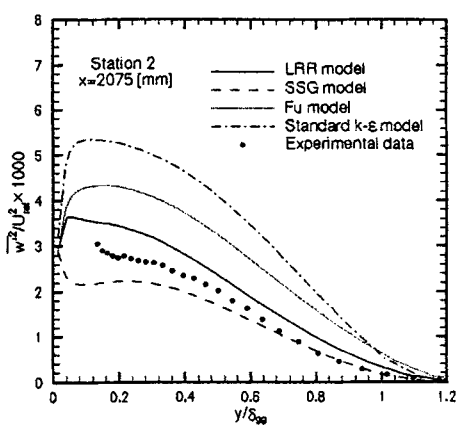

Fig. 11 Calculated results of normal stress $\overline{w'^2}$

predicted turbulent normal stresses in the bend region (Station 2) with the experimental data. Comparing Figs. 6 and 8 with Figs. 9 and 11, we can see that the turbulent normal stresses are

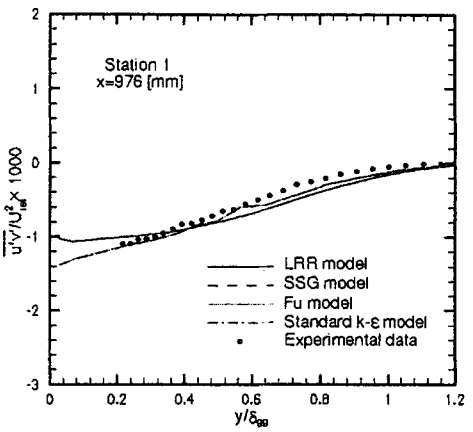

Fig. 12 Calculated results of shear stress $\overline{u'v'}$

increasing in the bend region because the additional rates of strain due to the spanwise pressure gradient increase the production of $\overline{u'^2}$ and $\overline{w'^2}$ stresses. Also, it is indicated from Fig. 7 and Fig. 10 that the increase in the $\overline{v'^2}$ stress without production is caused by the increase in the pressure-strain redistribution terms, resulting from increase of production of Reynolds normal stress $\overline{u'^2}$ and $\overline{w'^2}$. In fact, there is a strong anisotropy of turbulent structure due to the spanwise pressure gradient as pointed out by the experimental results. However, as shown in Figs. 9 to 11, the standard k-ε model can not predict anisotropy of normal stress-i. e. normal stresses are predicted to be roughly equal because this model is based on the isotropic eddy viscosity concept. Particularly, as shown in Fig. 10 and Fig. 11, normal stresses of $\overline{v'^2}$ and $\overline{w'^2}$ of the Fu model are considerably overpredicted because pressure-strain redistribution term of $\overline{v'^2}$ is overpredicted. Thus the standard k-ε and Fu models fail to capture the anisotropy of turbulent structure. On the other hand, the LRR and SSG models are effectively predicting the anisotropy of turbulent normal stresses although there are slight differences between the prediction and the experimental data.

The predicted and measured turbulent shear stresses $\overline{u'v'}$ in the upstream and bend regions are seen in Figs. 12 and 13. While the standard k-ε model fails to predict the anisotropy of shear stress, the results calculated by the LRR, Fu and SSG models closely agree with experimental data.

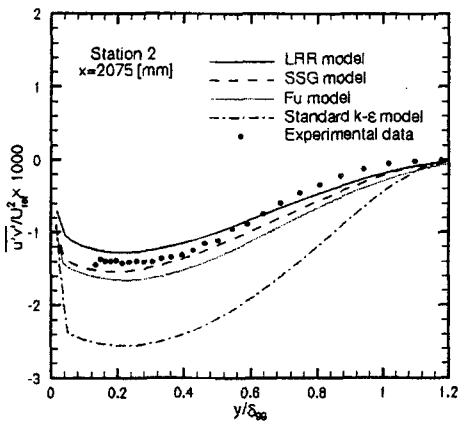

Fig. 13 Calculated results of shear stress $\overline{u'v'}$

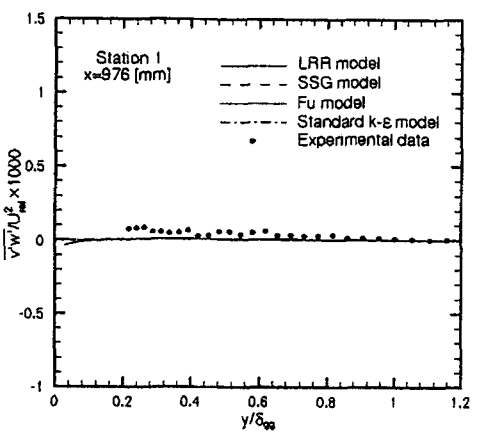

Fig. 14 Calculated results of shear stress $\overline{v'w'}$

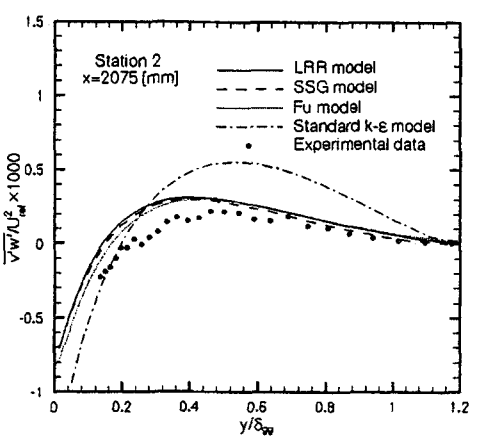

Fig. 15 Calculated results of shear stress $\overline{v'w'}$

It can be concluded from Fig. 12 and Fig. 13 that the shear stress $\overline{u'v'}$ is increased by additional rates of strain in the bend region.

Figures 14 and 15 represent the distribution of the Reynolds shear stress $\overline{v'w'}$ in the upstream and bend regions. The results of the LRR, Fu and SSG models closely agree with experimental data. However, there is a considerable disagreement between the prediction of the standard k-ε model and the experimental data, indicating that the standard k-ε model may produce inaccurate predictions for three dimensional turbulent flows driven by a pressure gradient. Physically, the shear stress $\overline{v'w'}$ is nearly zero as seen in Fig. 14 because of the 2DTBL in the upstream region. However, as shown in Fig. 15, the $\overline{v'w'}$ stress has the same order as the $\overline{u'v'}$ stress in the bend region because the $\overline{v'^2}$ stress, which is increased by the redistribution effect of pressure-strain, increases $\overline{v'w'}$ stress by increasing of $\overline{v'^2}\partial W/\partial y$ in production of the $\overline{v'w'}$ transport equation. This indicates the typical characteristics of 3DTBL, in which the $\overline{v'w'}$ stress should not be ignored.

5. Conclusions

In this article, numerical simulations using Reynolds stress models developed earlier were performed for 3DTBL driven by spanwise pressure gradient in a 30° bend. Comparisons of the results obtained by using the previous models of RSM and the standard k-ε model were made in the mean flow field and the turbulent structure. Following conclusions can be drawn.

(1) For the mean flow field, the calculated spanwise pressure gradient by the LRR model was in good agreement with the experiment data. However, there was some disagreement between the results obtained by using the models other than the LRR model and experimental data.

(2) The LRR and SSG models could produce more accurate predictions for capturing anisotropy of the turbulent structure than the Fu and standard k-ε models. Especially, the model of Fu produced inaccurate predictions for the turbulent normal stresses in the bend region. The Fu model is not effective in predicting the three-dimensional turbulent flows driven by the spanwise pressure gradient.

(3) The pressure-strain $\overline{u'^2}$ terms calculated by LRR, SSG and Fu models agreed closely with experimental data except in the near wall region. In contrast, the pressure-strain $\overline{v'^2}$ terms calculated by the LRR and SSG models were slightly overpredicted, Fu model was considerably overpredicted relatively.

(4) All models showed good prediction of pressure-strain redistribution terms in the outer layer, whereas all models failed to predict pressure-strain redistribution terms in the inner layer. This failure might be due to the turbulent modeling for the pressure-strain term. The models investigated in this paper were not capable of describing the non-local process existing in the inner layer since these models were intrinsically based on the local concept.

(5) The order of the $\overline{v'w'}$ stress was nearly same as order of the $\overline{u'v'}$ stress in the bend region. Which is a typical characteristic of 3DTBL. This $\overline{v'w'}$ stress resulted from the spanwise strain rate due to the pressure gradient and contributed to the increased production of the normal stresses.

The LRR and SSG models predicted turbulent normal stresses better than the Fu and the standard k-ε models. Nevertheless, the models of LRR and SSG did not effectively predict pressure-strain redistribution terms in the inner layer because the models of the pressure-strain term were based on the locally homogeneous approximation. Therefore, to give better predictions of the pressure-strain term, the way to bring non-local effect into the turbulence modeling for the pressure-strain term should be considered.

Acknowledgements

The research was supported by Chung-Ang University Grant in 1998.

References

Bradshaw, P. and Terrell, M. G., 1969, *The response of a turbulent boundary layer on an infinite swept wing to the sudden removal of pressure gradient*, NPL Aero Rep. 1305.

Durbin, P. A., 1993, *On modeling three-dimensional turbulent wall layers*, Phys. Fluids, A, 5 (5).

Flack, K. A., and Johnston, J. P., 1993, *The near-wall region of a detaching three-dimensional turbulent boundary layer*, Int. Conf. On Near-Wall Turbulent Flow, March 15-18, Tempe, Arizona.

Fu, S., 1988, *Computational modeling of turbulent swirling flows with second-moment closures*, Ph. D. Thesis, UMIST, Manchester, England.

Gibson, M. M. and Launder, B. E., 1978, *Ground effects on pressure fluctuations in the atmospheric boundary layer*, J. Fluid Mech. 86, 491~511.

Hogg, S. and Leschziner, M. A., 1989, *Second-momentum-closure calculation of strongly swirling confined with large density gradients*, Int. J. Heat and Fluid Flow, Vol. 10. No. 1, pp. 16~27.

Johnston, J. P., 1970, *Measurements in a three-dimensional turbulent boundary layer induced by a swept, forward-facing step*, J. Fluids Eng., Vol. 98, pp. 823~844.

Johnston, J. P., 1994, *Near wall flow in a three-dimensional turbulent boundary layer on the end wall of a rectangular bend*, AIAA 94-0405.

Jones, W. P. and Launder, B. E., 1972, *The prediction of laminarization with a two-equation model of turbulence*, International Journal of Heat and Mass transfer, vol. 15, pp. 301~314.

Launder, B. E., 1986, *Low-Reynolds-number turbulence near walls*, Rep., TFD/86/4, Dept. of Mech. Eng., UMIST.

Launder, B. E. and Spalding, D. B., 1974, *The numerical computation of turbulent flow*, Computer Method in Applied Mechanics and Engineering, Vol 3, pp. 269~289.

Launder, B. E., Reece, G. J. and Rodi, W., 1975, *Progress in the development of a Reynolds-stress turbulence closure*, J. Fluid Mech., 68, 537~566.

Lin, C. A., 1990, *Three-dimensional computations of injection into swirling cross-flow using second moment closure*, Ph. D. Thesis, UMIST, Manchester, England.

Reynolds, W. C., 1991, *Analytical methods in*

turbulence, ME261B course, Stanford University.

Rotta, J. C., 1979, *A family of turbulence models for three-dimensional boundary layers*, In Turbulent Shear Flows I Springer-Verlag, New York, 267~278.

Schwarz, W. R. and Bradshaw, P., 1992, *Three-dimensional turbulent boundary layer in a 30 degree bend: experiment and modeling*, Rept. MD-61, Thermosciences Division, Stanford University.

Spalart, P. R., 1988, *Direct simulation of a turbulent boundary layer up to* $Re_\theta=1410$, J. Fluid Mech. Vol. 187, pp. 61~98.

Speziale, C. G., Sarkar, S. and Gatski, T. B., 1991, *Modelling the pressure-strain correlation of turbulence: an invariant dynamical systems approach*, J. Fluid Mech., 227, 245~272.

Wilcox, D. C., 1993, *Turbulence Modeling for CFD*, DCW Industries Inc. Lacanada California.